Microstructural and mechanical characterization of laser beam welded AA6056 Al-alloy

Article *in* Materials Science and Engineering A · September 2011

DOI: 10.1016/j.msea.2011.06.010

4 authors:

Murat Pakdil
Bolu Abant Izzet Baysal University

Gürel Çam
Iskenderun Technical University

M. Koçak
Gedik Holding, Gedik University

S. Erim
Dokuz Eylul University

Materials Science and Engineering A 528 (2011) 7350–7356

Contents lists available at ScienceDirect

Materials Science and Engineering A

journal homepage: www.elsevier.com/locate/msea

Microstructural and mechanical characterization of laser beam welded AA6056 Al-alloy

M. Pakdil[a], G. Çam[b,*], M. Koçak[c,1], S. Erim[d]

[a] Abant Izzet Baysal University, Faculty of Engineering & Architecture, Bolu, Turkey
[b] Mustafa Kemal University, Faculty of Engineering, Iskenderun-Hatay, Turkey
[c] Gedik Welding Inc., Ankara Cad., 34913 Şeyhli, Pendik, İstanbul, Turkey
[d] Dokuz Eylül University, Faculty of Engineering, Bornova-İzmir, Turkey

ARTICLE INFO

Article history:
Received 7 May 2011
Received in revised form 5 June 2011
Accepted 6 June 2011
Available online 12 June 2011

Keywords:
Aluminum alloys
Laser beam welding
Strength undermatching
Mechanical properties
Fatigue

ABSTRACT

Laser beam welding is considered to be a suitable joining process for high speed, low distortion, and high quality fabrication of aircraft structures manufactured from aluminum alloys, which are mainly preferred due to their favourable properties, such as high strength to weight ratio, ease of forming and high thermal and electrical conductivity. However, the laser beam welding of 6000 series aluminum alloys may exhibit a tendency to solidification cracking, and porosity may be a major problem unless appropriate welding parameters and filler metal are employed.

In this study, the microstructural aspects and mechanical properties of laser beam welded new generation aluminum alloy, namely 6056, developed especially for aircraft structures, are investigated. A continuous wave CO_2 laser using AlSi12 filler wire was employed. A detailed microstructural examination of the weld region was carried out by Scanning Electron Microscopy (SEM). Standard tensile and microflat tensile specimens extracted from the welded plates were tested at room temperature for the determination of general and local mechanical properties of the welded joints. Extensive microhardness measurements were also conducted. Crack growth mechanisms of the joints produced were also determined by conducting fatigue tests under various stress ratios (i.e., $0.1 \leq R \leq 0.7$).

1. Introduction

In recent years, application areas of aluminum alloys have experienced a great increase; this in turn, stimulated intensive research activities on new generation aluminum alloys. Aluminum alloys possessing high strength, low weight and resistance to corrosion offer several advantages compared to the other commercial materials including steels.

Parallel to the increase in research on the weldability aspects of aluminum alloys, applications of welded aluminum structures are also expanding. In cases where it is not possible to manufacture an integral component by other production methods, one alternative solution can be the production of welded components, provided that the welding process is feasible and economically acceptable by the manufacturer. Therefore, weldability is an important factor for wide-spread application of a material.

Laser beam welding of specified aluminum alloys has been approved for a number of applications. These are mainly in the automotive, aerospace, construction, and electronics industries [1–6]. In aerospace industry, laser beam welding is being considered to be an alternative to mechanical fastening and adhesive bonding in certain applications. The recent commercial availability of high powered lasers has made it possible to consider welding as a practical alternative to riveting in the assembly of commercial aircraft structures. In compression dominated areas, such as the lower fuselage, the welded structure may be on the order of 10% lighter due to the more efficient use of stringer material, the favourable yield strength of candidate weldable alloys and the reduction of the amount of sealant and the number of fasteners [2].

The 6000 series aluminum alloys exhibit a tendency to solidification cracking unless the weld metal composition includes appropriate filler metal additions. Intergranular cracking in partially melted base metal adjacent to the weld fusion boundary (i.e., liquation cracking) is also a known problem in 6000 series arc welds [3–5,7].

The peak temperature in the heat affected zone (HAZ) causes varying amounts of grain coarsening and solution of the precipitates responsible for strengthening 6000 series alloys. Moreover, local as-welded microstructural features can be expected to reduce intergranular corrosion resistance. However, it is believed that a partial recovery of weldment strength and corrosion resistance can

* Corresponding author. Tel.: +90 535 7886978; fax: +90 326 2455499.
E-mail address: gurelcam@gmail.com (G. Çam).
1 Previously at HZG Geesthacht.

0921-5093/$ – see front matter © 2011 Elsevier B.V. All rights reserved.
doi:10.1016/j.msea.2011.06.010

be achieved by welding in the naturally aged condition, followed by an artificial aging heat treatment of the welded assembly [3].

When welding an age hardenable alloy, the HAZ can be thought of as two temperature zones. The lower temperature zone near the unaffected base material (BM) is exposed to temperatures just below the solvus line and overaging may take place, a process associated with the growth of equilibrium precipitates due to diffusion. In the higher temperature zone near the fusion zone (FZ) where the temperatures during welding exceed the solvus line, the respective phases are dissolved. Subsequently, at positions adjacent to the FZ higher peak temperatures are experienced and greater amount of dissolution of strengthening phases can occur. The higher temperature zone becomes solutionized eliminating the effects of age hardening [4–7]. Moreover, excessive porosity in aluminum welds can occur unless effective measures are taken prior to and during welding, to keep sources of hydrogen, such as moisture or organic compounds, away from the weld zone [8–10].

Compared to other conventional welding processes, such as arc welding, laser beam welding offers the benefit of a narrow heat affected zone that helps to minimize metallurgical problems that can arise from welding age hardened aluminum alloys. The low net weld heat input associated with this process results in rapid solidification rates in the fusion zone and lower peak temperatures in the adjacent base metal. Subsequently, this results in the formation of a narrow heat affected zones, and therefore, reduced thermal degradation of the adjacent base metal occurs [6–8].

Meeting the demand of the aerospace industry for a weldable fuselage skin alloy with equivalent static and dynamic properties, but with an improved resistance to intergranular corrosion (IGC), AA6056 alloy has been proposed [11,12]. Pechiney-patented 6056 alloy is an age-hardened, Al–Si–Mg–Zn–Cu–Mn alloy, developed to provide weldable thin extrusions with an excellent compromise on high strength and corrosion resistance [11,12]. 6056-T6 or -T78 sheet and thin plates are particularly suited for fuselage panels, especially when weldability and corrosion resistance are the key design characteristics.

In the present study, laser beam weldability of this weldable Al-alloy AA6056 was studied. Microstructural investigations and mechanical tests were conducted on the welded joint, in order to establish the local microstructure–property relationship. Macroporosity was detected in the weld region. Also, the influence of strength loss (undermatching) in the fusion zone on the local and global fracture behavior was determined. Fatigue crack propagation behavior of base metal and laser beam welded joint was analysed for *R* (stress ratio) ratios of 0.1, 0.3, 0.5, and 0.7. Fatigue crack propagation behavior of laser beam welded new generation aluminum alloy 6056 was examined and analysed in detail. Grain boundary liquation and porosity were determined in the weld regions of new generation aluminum alloys which were laser beam welded using AlSi12 weld wire. The effects of these common problems (grain boundary liquation and porosity) on fatigue crack propagation were investigated. Moreover, the relationship between *R* and porosity has been determined.

2. Experimental procedure

In this study, AA6056 Al-alloy plates of 6 mm thickness were joined by continuous wave CO_2 laser beam welding in the T6 heat treated condition using AlSi12 wire filler.

The plates have been butt-welded parallel to their rolling directions. The filler wire used (AlSi12) is 1.2 mm in diameter. Microstructural examinations were carried out using SEM. Extensive microhardness measurements were conducted across the weld region including the HAZ and base metal from three different locations, namely top, middle and bottom as shown in Fig. 1. Energy-dispersive X-ray spectroscopy (EDX) analyses were also conducted in the BM, FZ and the HAZ of the joint to determine the chemical compositions of the respective areas.

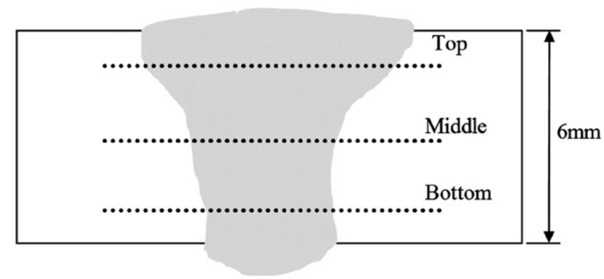

Fig. 1. Schematic showing the positions where microhardness measurements conducted.

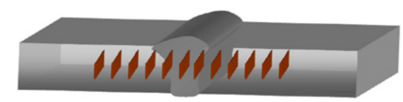

Fig. 2. Micro-flat tensile specimen cutting plan.

Standard tensile specimens were extracted from the base metal (both in LT and TL directions, that is, parallel and normal directions to the rolling direction) and from the welded joint. These specimens (3 specimens for each condition) were tested at room temperature to determine the effect of laser beam welding on global fracture behavior of the plate. Micro-tensile specimens extracted from the three different regions of the joint, namely BM, FZ and HAZ (Figs. 2 and 3) were tested to determine the local mechanical property changes resulting from laser beam welding. The micro-flat tensile tests were conducted at a rate of 0.4 mm/s. Fatigue crack propagation (FCP) mechanisms of this new generation 6056-T6 series aluminum alloy, joined with a CO_2 laser using AlSi12 filler wire, were also determined experimentally.

3. Results and discussion

3.1. Microstructural and hardness aspects

X-ray analyses were conducted to identify the general problem of porosity in the FZ of CO_2 laser beam welded aluminum alloys. It was found that there is a considerable amount of small-sized porosity (i.e., $\leq$1 mm in size) in the weld seam.

Fig. 4 shows a macrograph of laser beam welded Al-alloy 6056 joint obtained in this study, illustrating also that porosity exists in the fusion zone, which is quite usual in Al-alloys. The microstructure of the FZ consisted of fine grained dendritic microstructure with Si, Cu and Mg rich precipitates at the grain boundaries. The reason for the formation of this fine grain microstructure in the

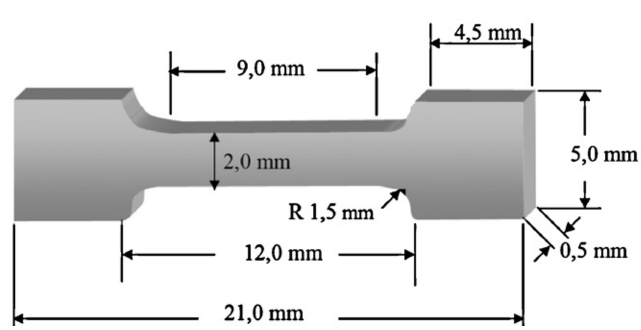

Fig. 3. Micro-flat tensile specimen dimensions.

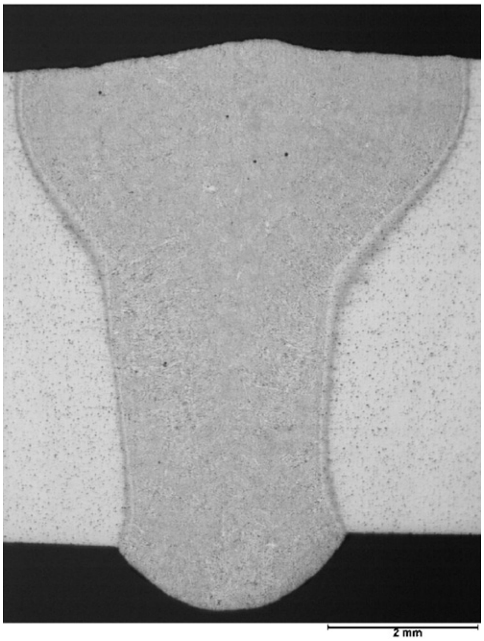

Fig. 4. Optical macrograph showing the cross-section of laser beam welded joint obtained.

FZ is the high solidification rates involved in power beam welding, which helps retaining the strength of the re-solidified aluminum [5–7]. No solidification cracking or liquation cracking occurred in the FZ or in the HAZ (Fig. 5), which are quite usual in arc welding of aluminum alloys. This can also be attributed to the higher cooling rates involved in laser beam welding. Moreover, owing to the higher cooling rates, a narrow HAZ has been formed and the coarsening of the strengthening precipitates in the HAZ is not that pronounced as it is the case in arc welding, where a higher extent of diffusion takes place due to the higher heat input during welding. There was, however, some liquation at the grain boundaries in the FZ and HAZ (Fig. 5).

The microhardness profiles obtained from three different locations (Fig. 1) are given in Fig. 6. As illustrated, a hardness decrease (strength undermatching) was observed in the HAZ and the FZ, the hardness minimum lying in the FZ in contrast to arc welding, where the hardness minimum lies in the overaged HAZ region [13,14]. The reason for the hardness decrease in the HAZ is due to the fact that overaging takes place as a result of heat input during welding, which is usual for 6000 series Al-alloys. However, the hardness decrease in the HAZ was much lower than that of the HAZ formed in arc welds of the same plate [4–7]. The hardness level of the FZ was found to be restored to that of the HAZ, which can be attributed to the use of Si-containing filler wire, which changes the chemistry of the weld pool, and also to the relatively higher cooling rates associated with laser beam welding. Although a Si-containing filler wire was used to recover the strength, a hardness loss still occurred in the FZ.

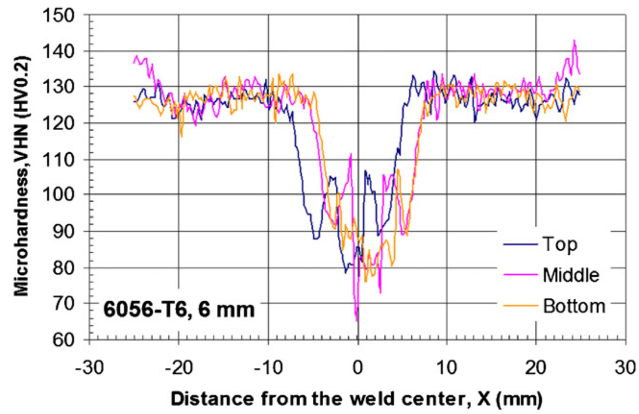

Fig. 6. Microhardness profile of the weld joint at T6 condition.

EDX analyses results are presented in Table 1. Figs. 7–9 illustrate the positions where EDX analyses were conducted. The grain boundaries in the FZ were found to be rich in Si, Cu and Mg suggesting that the segregation of alloying elements (already existing in the base plate and added with the filler wire) to grain boundaries. The hardness decrease in the FZ of the joint can be attributed to the loss of strengthening phases and the segregation of Si to the grain boundaries eliminating the solid solution hardening, which are the dominant strength-determining mechanisms in the FZ. On the other hand, the overaging is the most dominant strength-determining mechanism in the HAZ. The grain boundary segregation was also detected at the HAZ. However, the Si-content of the grain boundaries at the HAZ (about 1 wt.%) is much lower than those of the FZ (about 7 wt.%), where the increase of Si-content is due to the use Si-containing filler wire which changed the chemistry in the weld pool. However, the less pronounced hardness decrease in the HAZ in comparison to arc welding can be attributed to the lesser extent of overaging in laser beam welding.

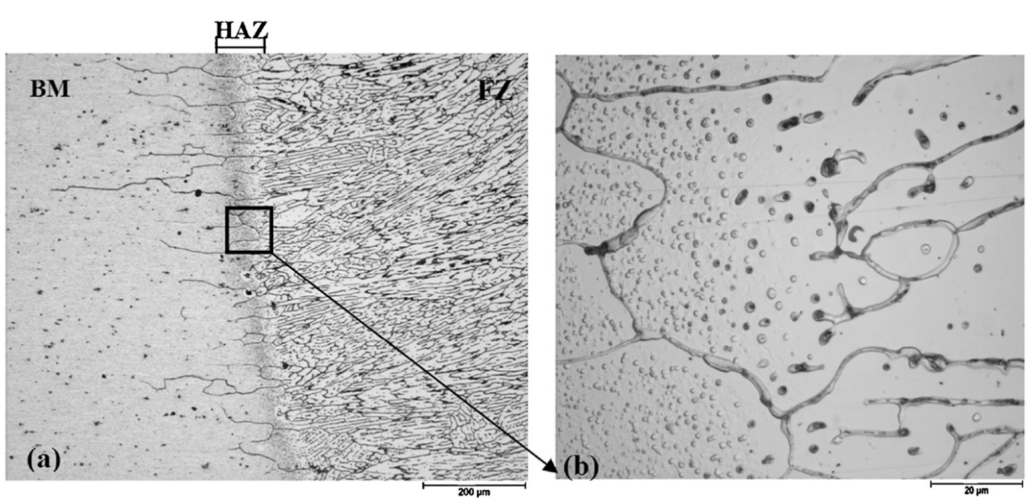

Fig. 5. Optical micrographs showing the HAZ in detail: (a) the edge of the fusion zone and (b) the details of the HAZ marked by square in (a).

Table 1
Chemical analyses results conducted in the welded joint in various regions, namely BM, HAZ and FZ.

Position[a]		Element (wt.%)					
		Cu	Mg	Mn	Fe	Si	Al
FZ	a_1	0.555	1.249	0.282	0.079	1.422	96.412
	a_2	2.944	3.167	0.615	0.402	7.292	85.580
	a_3	0.270	0.961	0.399	0.093	0.124	98.144
HAZ	a_1	1.081	1.924	0.273	0.155	1.112	95.454
BM	a_1	0.589	1.416	0.261	0.080	0.449	97.205
	a_2	0.656	1.329	0.174	0.054	0.352	97.434

[a] See Figs. 7–9.

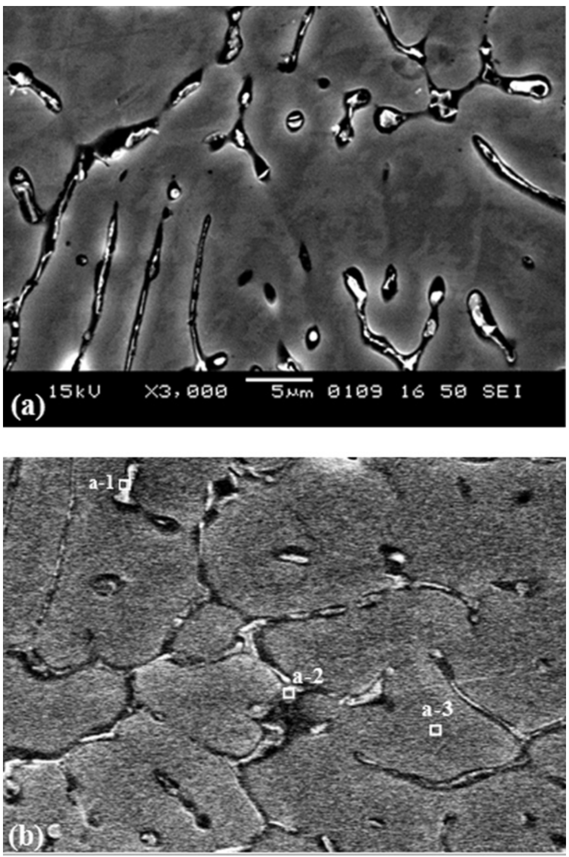

Fig. 7. SEM micrographs showing: (a) the microstructure of FZ and (b) positions where EDX analyses conducted.

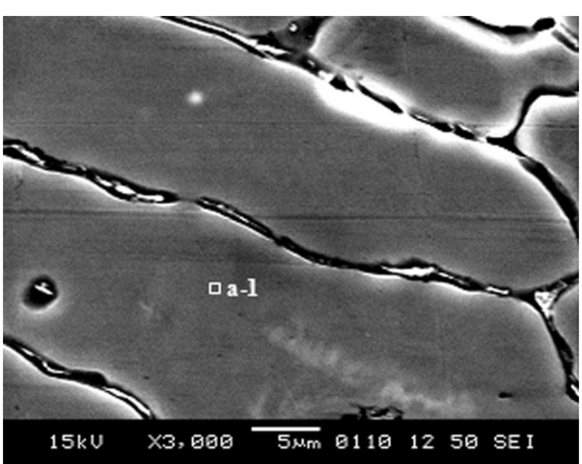

Fig. 8. SEM micrograph of the HAZ showing the EDX analysis point.

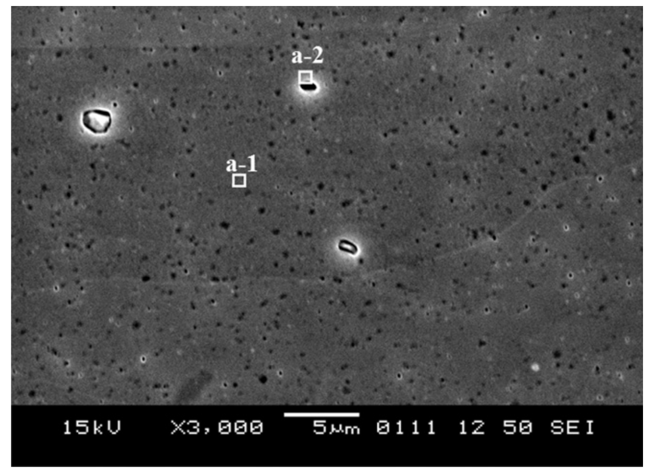

Fig. 9. SEM micrograph of the BM showing the analysis points.

3.2. Tensile properties

Global tensile properties of the laser beam welded joint were determined by testing conventional flat transverse tensile specimens at room temperature. The results are summarized in Table 2 and Fig. 10, which also includes the base metal properties both in LT and TL directions. The yield strength of the base plate was found to be the same value (i.e., 347 MPa) both in LT and TL directions, whereas the tensile strength varied slightly, being 362 and 371 MPa in LT and TL directions, respectively. The elongation of the BM also

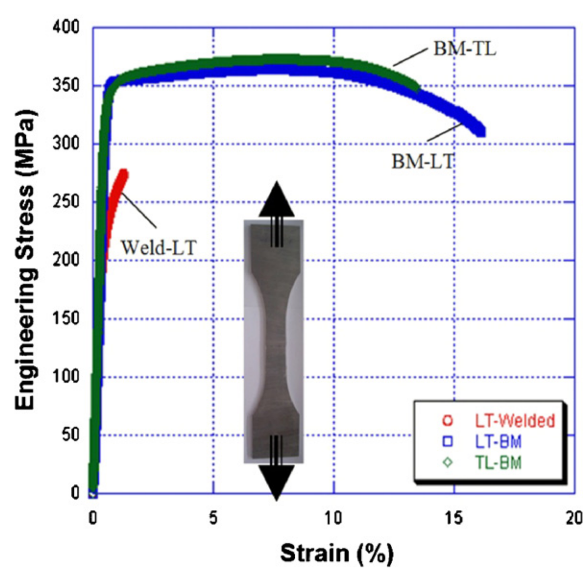

Fig. 10. Stress-strain curves from the BM (both in LT and TL directions) and weld joint specimens.

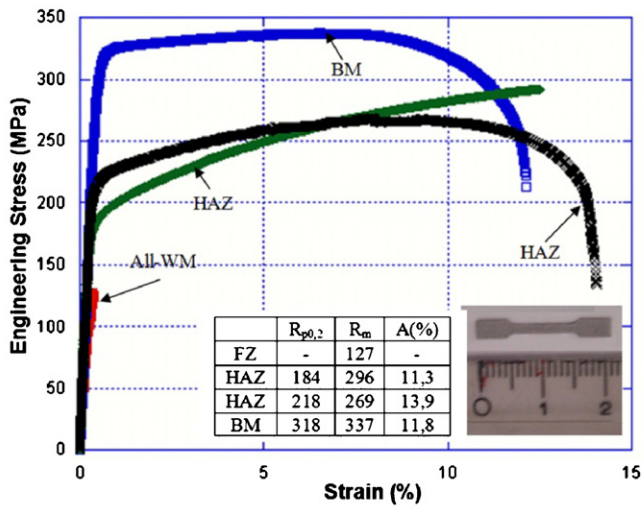

Fig. 11. Stress–strain curves obtained from the base metal and all-weld metal flat microtensile specimens.

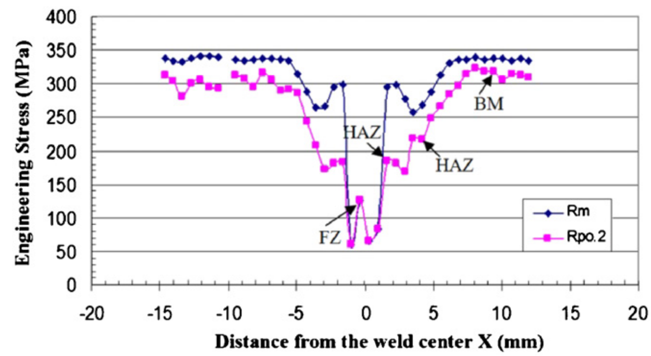

Fig. 12. Tensile property profiles of the welded joint obtained from micro-flat tensile specimens.

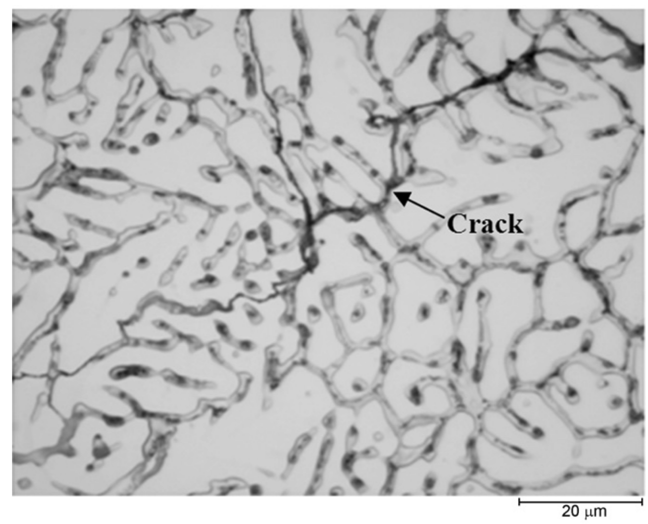

Fig. 13. FCP path in TL–welded specimen.

varied slightly with the change of the direction of the specimen with respect to the rolling direction, being 3% higher when tested parallel to the rolling direction.

All transverse tensile specimens extracted from the joint failed in the weld region due to the strength undermatching condition (the strength loss in the weld region, see the hardness profiles, Fig. 6). The joint efficiency in terms of yield and tensile strengths was about 65% and 75%, respectively, being relatively high compared to literature data [4–7,13,14]. On the other hand, transverse tensile test results showed significant losses in ductility, owing to strain concentration in the lower strength weld region, as expected from the hardness profile of the joint, Fig. 6. Thus, the joint efficiency in terms of elongation was quite low, being about 6%, which is not unusual due to the significant strength undermatching encountered in power beam welding of age-hardenable Al-alloys [4–7,13,14]. In undermatching cases, the stress concentration and consequent failure (confined plasticity) occur in the lower strength weld region of the joint, leading to an increased constraint within the weld region, and thus, significantly lower elongation values [13,14].

Micro-tensile specimens extracted from the three different areas of the joint (the BM, FZ and HAZ) were tested to determine the local mechanical characteristics. The results are presented in Fig. 11. The yield strength of the all-weld metal microtensile specimen was found to be 226 MPa, whereas that of the base material (BM) was 347 MPa, yielding a mismatch ratio of 0.65. This value is reasonable high compared to the data in the literature for laser beam welded age-hardenable Al-alloys joints. Moreover, the tensile properties of the base plate determined by standard macro- and non-standard micro-tensile specimens are in accordance with each other.

The tensile property profiles of the welded joints were also obtained by testing flat microtensile specimens and are illustrated in Fig. 12. The variations in strength values in the weld zone are in good agreement with the hardness results (see Figs. 6 and 12). Furthermore, these values are consistent with transverse tensile specimen results (see Fig. 10).

3.3. Fatigue crack propagation (FCP) test

As seen in Fig. 4, porosities were identified. To study the effect of these porosities on FCP, the following tests were undertaken:

Table 2
Tensile properties of Al6056-T6 base material both in LT and TL directions and the welded joint (bold characters are the average values).

Specimen	$R_{p0.2}$ (MPa)		R_m (MPa)		A (%)	
6056 T6-LT	348	**347**	363	**362**	16.3	**16.0**
	345		360		15.8	
	348		362		16.1	
6056 T6-TL	348	**347**	372	**372**	13.8	**13.2**
	345		371		13.0	
	348		372		12.9	
6056 T6 (LB welded joint)	225	**226**	275	**275**	0.9	**0.9**[a]
	225		276		0.9	
	227		275		0.9	

[a] Due to the presence of highly undermatched fusion zone.

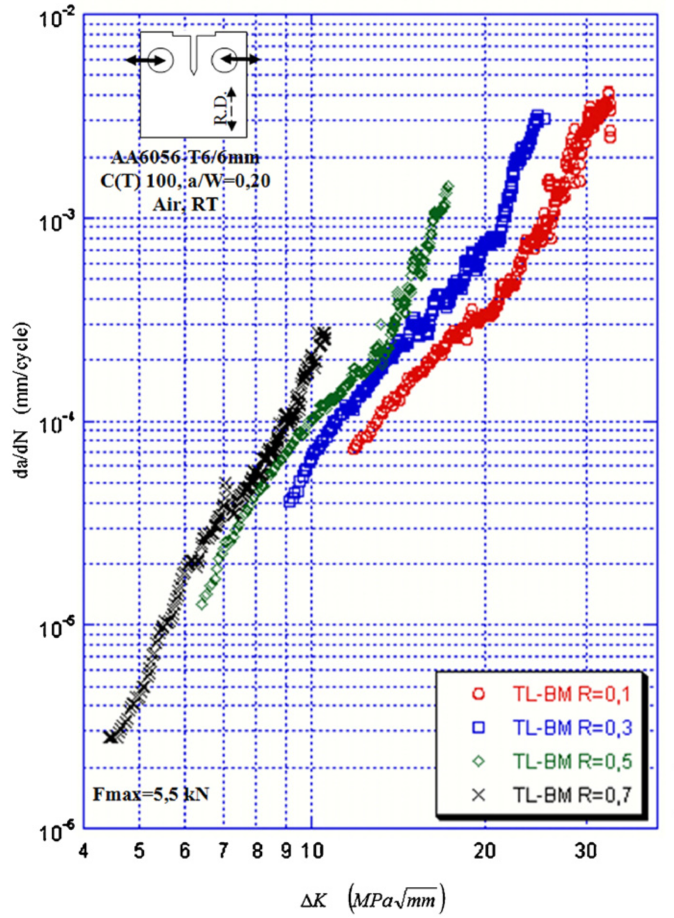

Fig. 14. d*a*/d*N* – Δ*K* curves of TL–BM specimens.

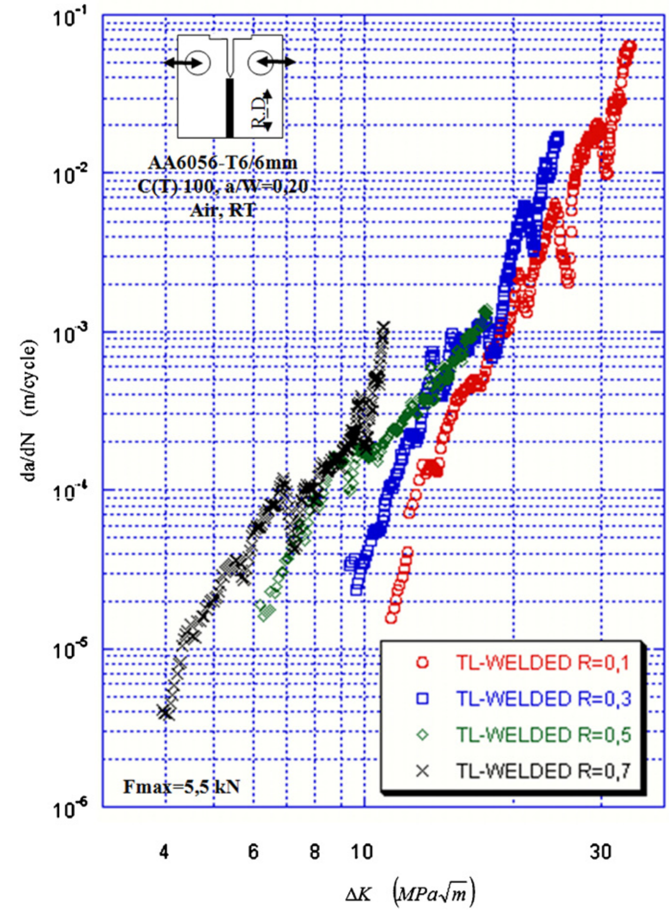

Fig. 15. d*a*/d*N* – Δ*K* curves of TL–welded specimens.

All of the fatigue crack propagation tests were conducted in accordance with ASTM E647. C(T) 100-type specimens were selected for the FCP tests, the reason being that C(T) 100-type specimens allow for better examination of the effect of porosity compared to C(T) 50-type specimens. Fatigue tests were conducted under various stress ratios (i.e., $0.1 \leq R \leq 0.7$). Effects of microstructural changes on crack growth mechanism were also investigated. Furthermore, the effect of grain boundary liquation in addition to the effects of stress ratio and porosity size, on the crack growth mechanism, was also determined. The results have shown that sound joints have been achieved by laser beam welding [15].

Fatigue crack propagation during testing was measured both with a crack opening mouth displacement (CMOD) clip and electrical potential drop (EPD) technique; in which the increase in crack length has been transferred to the computer during testing. Moreover, the crack length was measured by digital microscopes from both sides after the testing and the three measurement values have been compared with each other.

Appropriate parameters to be applied to TL–BM and TL–welded C(T) specimens were calculated separately according to ASTM 647 Norms. The maximum load, the frequency and other related parameters for valid crack lengths (between $0.20 \leq a/W \leq 0.60$) were calculated. As a result of these calculations, the applied frequency was chosen as 10 Hz in all FCP tests, the maximum load was 5.5 kN and all tests were conducted in air at room temperature.

The crack propagation occurs as a result of void formation and their coalescence typical in ductile fracture mechanism in BM specimens. The crack propagation mechanism in the welded region, on the other hand, is observed to be due to intergranular propagation along the grain boundaries (see Fig. 13).

When the graphics given in Figs. 14 and 15, drawn according to the Paris–Erdogan equation, are compared, the effect of porosity can be observed [15,16]. What is of interest in Fig. 14 and other fatigue diagrams is the instant variations in the fatigue curves of TL welds and decrease in crack propagation as a result of these variations. Porosity is thought to be the cause of this decrease.

4. Conclusions

In the present study, the microstructural aspects and mechanical properties of CO_2 laser beam welded 6056 aluminum alloy using AlSi12 filler have been investigated. The favourable results for manufacturing of such aluminum alloys by laser beam welding are expected, however, with such thickness of the material as used in the present study, the following results obtained show the merit of the present work. It is shown that high quality joints could be obtained in laser beam welding of 6056 Al-alloy plate using AlSi12 filler wire although some acceptable amount of porosity was present due to the hydrogen entrapment. Although grain boundary liquation was detected in the FZ and HAZ, no liquation cracking was observed. Another important observation to note is that the grain boundary liquation becomes more pronounced as the amount of Si along the grain boundaries increased. The overaging in the HAZ region of the welding leads to a decrease in the strength of HAZ while the strength of the FZ is restored to the level of the HAZ by using Si-containing filler wire. In the present study, higher mismatch ratios of the joints could be achieved when compared to the data in the literature for power beam welded age-hardenable Al-alloys joints.

Another important aspect of the present article is the determination of the crack growth mechanisms of the joints obtained with fatigue tests under various stress ratios; indeed typical ductile crack propagation mechanism is observed in the fatigue tests of TL–BM specimens while intergranular crack propagation is detected in the TL–welded specimens. However, as this study has clearly shown, the presence of porosity retards the crack propagation and slows down the crack propagation rate in relation with the value of *R*. When joining two parts, if the part that may cause the crack initiation (such as welding) is joined transverse to the rolling direction, fatigue crack propagation may proceed slower.

Acknowledgements

This work has party been conducted at the HZG-Geesthacht during the stay of Mr. Pakdil at this research center and hence the contribution of HZG-Geesthacht is highly acknowledged. The authors also wish to thank Dr. W.V. Vaidya, M. Horstmann, and P. Fischer (HZG-Geesthacht) and Ç. Yeni (Dokuz Eylul University, İzmir, Turkey) for their help in testing and evaluations. Thanks should be extended to Mr. J. Hackius for the provision of welded panels.

References

[1] C.M. Allen, Laser welding of aluminium alloys – principles and applications, TWI Report TWI, Abington, UK, 2004.
[2] B. Lenczowski, Proceedings of new lightweight alloys for welded aircraft structure. ICAS2002 Congress, Germany, 2002.
[3] B.R. Leigh, C. Poon, N. Ferguson, Proceedings of New Lightweight Alloys for Welded Aircraft Structure, ICAS2002 Congress, Germany, 2002.
[4] T.A. Marsico, R. Kossowsky, Laser Material Processing, ICALEO'89, vol. 69, Orlando, USA, 1989, pp. 61–71.
[5] D.L. Olson, A. Wahid, D.K. Matlock (Eds.), ASM Handbook, Volume 6: Welding, Brazing and Soldering, ASM International, Materials Park, Ohio, USA, 1993.
[6] G. Çam, J.F. dos Santos, M. Koçak, Laser and electron beam weldability of Al-alloys: Literature Review, GKSS 97/E/25, GKSS Research Center, Geesthacht, Germany, 1997, IIW Doc. IX-1896-98.
[7] G. Çam, M. Koçak, Int. Mater. Rev. 43 (1998) 1–44.
[8] A. Haboudou, P. Peyre, A.B. Vannes, G. Peix, Mater. Sci. Eng. A 363 (2003) 40–52.
[9] G. Çam, M. Koçak, J. Mater. Sci. 42 (2007) 7154–7161.
[10] B. Lenczowski, Proceedings of New Lightweight Alloys for Welded Aircraft Structure, ICAS2002 Congress, Germany, 2002.
[11] P. Rhenalu, 6056-T6/-T78 New Alloy—Sheets and Thin Plates—A Weldable Corrosion Resistant Low Density Alloy, Report, France, 2001.
[12] R. Dif, Ph. Lequeu, T. Warner, B. Bès, H. Ribes, Ph. Lassince, Recent developments in aluminum sheet alloys used in aerospace, Report, France, 2002.
[13] G. Çam, V. Ventzke, J.F. dos Santos, M. Koçak, G. Jennequin, P. Gonthier-Maurin, M. Penasa, C. Rivezla, Pract. Metallogr. 37 (2000) 59–89.
[14] G. Çam, V. Ventzke, J.F. dos Santos, M. Koçak, G. Jennequin, P. Gonthier-Maurin, Sci. Technol. Weld. Join 4 (1999) 317–323.
[15] M. Pakdil, G. Çam, S. Erim, Proceedings of 12th International Materials Symposium (IMSP'2008), October 15–17, 2008, Denizli, Turkey, 2008, pp. 469–479.
[16] P.C. Paris, F.A. Erdogan, J. Basic Eng. Trans ASME Ser. D 85 (1963) 528–534.